ORIGINAL ARTICLE

Experimental investigation of rheological behaviour and stability of mud system using novel image processing application in presence of activated carbon and silica-coated iron oxide nanoparticles

Shaine Mohammadali Lalji[1] · Syed Imran Ali[1] · Rezwan Ullah[2] · Syed Muhammad Ali[3] · Yassar Kamal Zia[3] · Rizwan Ghauri[4] · Abrar Ahmed[5]

Abstract

The success of any drilling activity is mainly dependent on the behaviour of the drilling fluid. These fluids not only act as a primary barrier but are also responsible for maintaining hole integrity, carrying and lifting the drilled cutting and preventing the fluid loss. All these characteristics can be achieved by the help of desired rheological properties. Silica-coated iron oxide nanoparticles (0.25 and 0.5 wt. %) and activated carbon (0.25 and 0.5 wt. %) are being utilised in this study to formulate stable and high-performance water-base drilling fluids. The rheological characteristics of the mud system were investigated using different rheological parameters that consist of plastic viscosity, yield point, apparent viscosity and gel strength. On the other hand, the stability of the mud systems was observed with the help of intensity profile plots and interactive 3D surface plots using image processing technique. It is a novel method of spotting the changes in mud stability under no circulation condition. The results of the study reveal that all the muds showed pseudo-plastic shear thinning behaviour with flow index < 1. No substantial changes in mud density were recorded after the addition of these particles. The maximum mud weight of 8.8 ppg was recorded in activated carbon samples. All the rheological properties were obtained at ambient conditions of 27 °C. It was observed that samples 1 and 4 demonstrate rheological characteristics in the desired operating range with optimum yield point-to-plastic viscosity ratio in range of $0.75–1 \frac{lb/100ft^2}{cP}$. This ratio indicates that the concentration of both the particles is the key factor in achieving desire cutting carrying capacity. Moreover, according to intensity profile plots for the determination of mud stability, the sample with least concentration of activated carbon was the most stable sample. No substantial change in stability was recorded in that sample after two days of experimentation. On the contrary, silica-coated iron oxide nanoparticles start to de-phase on Day 1, and separation was quite visible on Day 2. On Day 5 of the stability test, it was perceived with the help of 3D surface plots that each sample was undergoing either solid settling phenomenon or dephasing. Based on the findings of the study, it can be concluded that activated carbon because of its high surface area and nontoxic behaviour can act as an efficient additive in terms of maintaining the rheological properties and stability of water-based mud system.

Keywords Activated carbon · Image processing · Intensity profile plot · Interactive 3D surface plots · Rheological properties · Silica-coated iron oxide nanoparticle

Abbreviations

WBM	Water-based mud
OBM	Oil-based mud
WBDF	Water-based drilling fluids
SEM	Scanning electron microscope
cc	Centimetre cube
mL	Millilitre
g	Grammes
PV	Plastic viscosity
YP	Yield point
AV	Apparent viscosity
GS	Gel strength

Extended author information available on the last page of the article

Introduction

Drilling fluid is a vital component in any drilling process (Aftab et al. 2017). In this regard, the right choice of drilling fluid with proper additives is a crucial factor for successful

drilling activity (Ali Esfandyari Bayat et al. 2018). Drilling muds are used for numerous functions which include reducing the friction by increasing lubrication, lifting and carrying the cutting up to the surface, maintaining hydrostatic head in the wellbore, providing seal against a permeable formation, and minimising the hole roughness and eliminating corrosive environment (Aftab et al. 2017; Ali Esfandyari Bayat et al. 2018; Elkatatny 2019; Lalji et al. 2021a, b; Kamath et al. 2022; Mohan et al. 2022). In general, drilling fluids are classified into three distinct categories, namely oil-based mud system (OBM), water-based mud system (WBM) and synthetic mud systems (Sharma et al. 2012). The synthetic mud systems and oil-based mud systems have some high operational, cost and environmental problems as compared to water-based mud systems (Al-Arfaj et al. 2014; Ali Esfandyari Bayat et al. 2018). Therefore, WBM is counted as the preferred option in spite of its limitations. Hence, it is imperative to study the properties of WBM for the purpose of improving its properties.

There are various drawbacks associated with water-based drilling fluids (WBDF) that include wellbore stability as a result of shale swelling, poor rheological properties, and high loss of filtrate volume that eventually gives rise to some severe differential pipe sticking problems (Al-Ansari et al. 2017; Adnan Aftab et al. 2020). These problems can be minimised using the OBM systems. However, environmental issues prohibited its use (Adnan Aftab et al. 2020). Therefore, WBM systems were counted as the main solution to the above-mentioned problems. These were the reasons that provoked researchers to concentrate on the modifications of properties of WBM systems, especially its rheological behaviour. The characteristics of WBM can be controlled and improved through the use of different additives that are mainly classified as salt, polymers and nanoparticles.

The distinctive properties of nanomaterials assist them to become part of a variety of disciplines (Chen and Huang 2021; Cheng et al. 2022; Duan et al. 2022; He et al. 2022; Shao et al. 2022; Si et al. 2022; Soares et al. 2022; Xie 2022a, 2022b; Zhang et al. 2022; Zhu et al. 2022; Qin et al. 2023). However, the addition of nanoparticles in the drilling industry has now opened new doors for the petroleum sector, and it is thought to be the most recent development in the oil and gas field. These materials are responsible for improving mechanical, rheological and thermal properties of mud systems (Abdo and Haneef 2013). Performances of different nanomaterials in drilling muds are studied by numerous researchers (Jung et al. 2011; Al-saba et al. 2018; Mohideen 2019; Lalji 2022a, 2022b). Modifications in the properties of drilling mud by the use of nanoparticle ultimately help the industry to minimise the non-productive time events.

Iron oxides, as a result of their technological significance, are considered to be the most significant transition metals (Asab et al. 2020). Magnetite (Fe_3O_4) is the most common iron oxide that is found in nature, and it also possesses some interesting characteristics (Babay et al. 2015; Asab et al. 2020). This oxide of iron consists of two valence states Fe^{2+} and Fe^{3+}. However, its nanoparticle undergoes two major problems like oxidation in the presence of air, and second, rapid cluster formation (Babay et al. 2015). Therefore, coating the surface of iron oxide particle is the most common solution that can easily confront these above-mentioned problems (Babay et al. 2015). The coating can be through organic materials like alginate and dextran (Turrina et al. 2022), or it can be done with the help of inorganic material such as silica (Turrina et al. 2022). The inorganic coating with silica has now become a promising approach in order to improve the characteristics of iron oxide nanoparticles (Yong-Hui Deng et al. 2005). Silica coating layer is utterly responsible for developing a chemically inactive surface in the presence of any biological systems (Yong-Hui Deng et al. 2005); however, the problem of agglomeration is still associated with this material. Consequently, the rheological properties and the stability of drilling fluid need more suitable materials.

The carbonaceous materials are other segments of compounds that are widely used in different commercial sectors. In the form of nanoparticles, these carbonaceous materials are generally classified into two separate categories—carbon nanoparticles and graphene nanoparticles. Their distinctive mechanical, physical and chemical behaviours enable the researchers to not only use them in pristine form but also encourage their use in different composite forms as well (Ibrahim Khan and Khan 2019). Their commercial applications include: fillers, sensing technologies and electronic devices (Chen et al. 2022; He et al. 2022; Tiwari Nidhi 2022; Wang et al. 2022a, 2022b; Xie et al. 2022a, b; Yan et al. 2022; Zhang et al. 2022; Kuang et al. 2023). However, poor dispersion of these particles in the water-base mud system is one of the serious problems associated with them (Cheraghian 2021). Therefore, the focus in this study is on activated carbon, another carbonaceous material with high adsorption capacity and fast reaction kinetics.

Activated carbon is defined as a porous carbonaceous material with some unique properties (Heidarinejad et al. 2020). This material has some vast applications in the field of wastewater treatment, desalination and air purification (Kosheleva et al. 2019; Heidarinejad et al. 2020; Ahmadi et al. 2021; Deng et al. 2021a, 2021b, 2022; Sun et al. 2021; Lu et al. 2022; Choi et al. 2023). 90% of this material is made from carbon (Samsuri et al. 2014; Heidarinejad et al. 2020). In addition, this compound contains high surface area with different associated functional groups that are mainly responsible for adsorption of any contaminants (Heidarinejad et al. 2020; Begum et al. 2022). Azeem et al. bind the activated carbon with polyamine dendrimers and use the compound for shale swelling inhibition (Azeem Rana 2022). The larger surface area, the nontoxic nature and the nano-carbon content

related to activated carbon help it to bind effectively, which in turn enhances the drilling mud properties (Azeem Rana 2022). Limited applications of activated carbon in drilling are available in literatures; therefore, it is important to focus on this material in order to investigate its performance.

In the current study, for the first time, the rheological comparison is done between silica-coated iron oxide nanoparticles and activated carbon. To the best of our knowledge, this is the first rheological and mud stability comparison study for these two particles. Two different concentrations of each particle were investigated, and based on that all, the rheological parameters were obtained. In addition, for the first time, stability of the mud system was observed with the help of intensity profile plots and interactive 3D surface plots. The mud samples were kept stationary for the duration of five days, and based on that, different intensity plots were obtained. These plots show the settling and the dephasing of each sample after five days. It is a novel method for spotting the changes in mud stability when there is some circulation for any unknown event.

Materials and methods

Materials

The study aims to investigate rheological behaviour and stability of the mud system after the addition of activated carbon and silica-coated iron oxide nanoparticles. Activated carbon is attained from the chemical treatment of different carbonaceous resources. During this study, this compound was purchased from Sigma Aldrich. On the other hand, silica-coated iron oxide nanoparticles are the nanoparticles of iron oxide coated with silica. The purpose of this coating is to increase the force of repulsion between the iron oxide particles.

Scanning electron microscope (SEM) imaging of particles

Figure 1a, b shows the scanning electron microscope imaging (SEM) for both the particles in the study. The SEM instrument is manufactured in Japan by Joel, and the model used during the analysis is JSM 6380A. Figure 1a is the SEM imaging of activated carbon. It can be observed that the external surface of activated carbon consists of holes, cracks and fissures. Additionally, there are also some small fine particles over its surfaces, which are likely to be the ash particles (Fronczak et al. 2019). Figure 1b shows the SEM imaging of silica-coated iron oxide nanoparticles. It can be observed from the figure that the particles are spherical in shape just like magnetic beads.
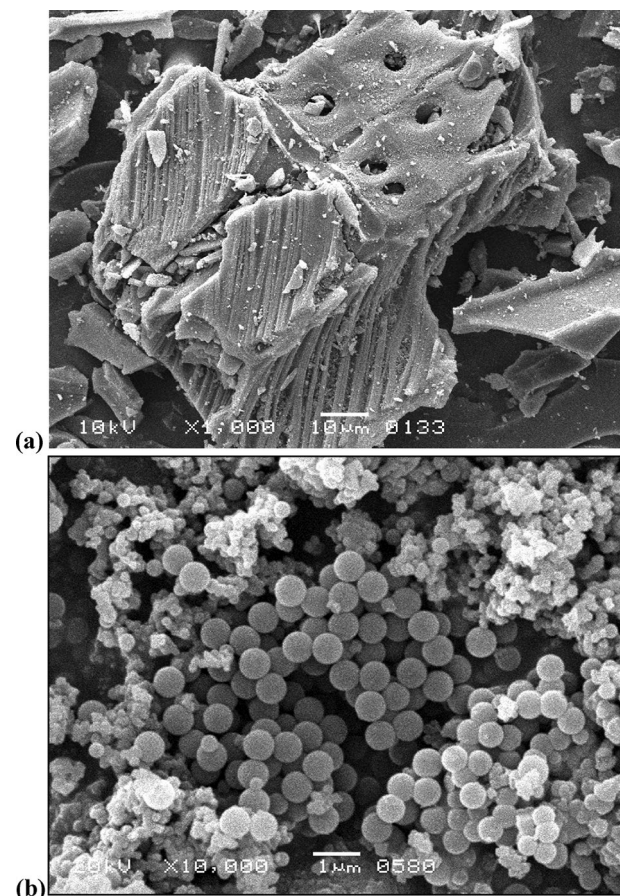

Fig. 1 a, **b** SEM imaging of particles a activated carbon b silica-coated iron oxide nanoparticles

Preparation of water-based drilling fluid

During this study, 350 cc of salt polymer amine water-based drilling mud was prepared and tested. Table 1 shows the additives, quantity and its supplier used to prepare the base mud system.

The purpose of this study is to investigate the rheological variation in salt polymer amine water-based drilling mud after the addition of nanoparticle and a carbon-supported particle. The particles are added into two different concentrations (0.25 wt. % and 0.5 wt. %) respectively. In addition to rheological behaviour, the stability of the mud systems was also investigated using the image processing software. 10 mL of each mud sample was placed in the test tube after the addition of particles. These samples were monitored three times during the course of five days. The intensity profiles of the test tubes were recorded for each day, and the settling of the particles was observed based on the profile. Figure 2 shows the flowchart of the study conducted in this article. Table 2 shows four samples with their concentrations that are used in this work.

Table 1 Additives used to prepare the water-based drilling mud

Additive name	Quantity	Unit	Supplier
Tap water	306	mL	–
Sodium carbonate (Na_2CO_3)	0.25	G	Service company operating in Pakistan
Potassium chloride (KCL)	26	G	Service company operating in Pakistan
Xanthan gum	1.5	G	Service company operating in Pakistan
Amine solution	10.5	mL	Service company operating in Pakistan
Barite	80	G	Service company operating in Pakistan
Nanoparticle	0.875 and 1.75	G	Service company operating in Pakistan
Activated carbon	0.875 and 1.75	G	Sigma Aldrich

Fig. 2 Flowchart of the work conducted in this study
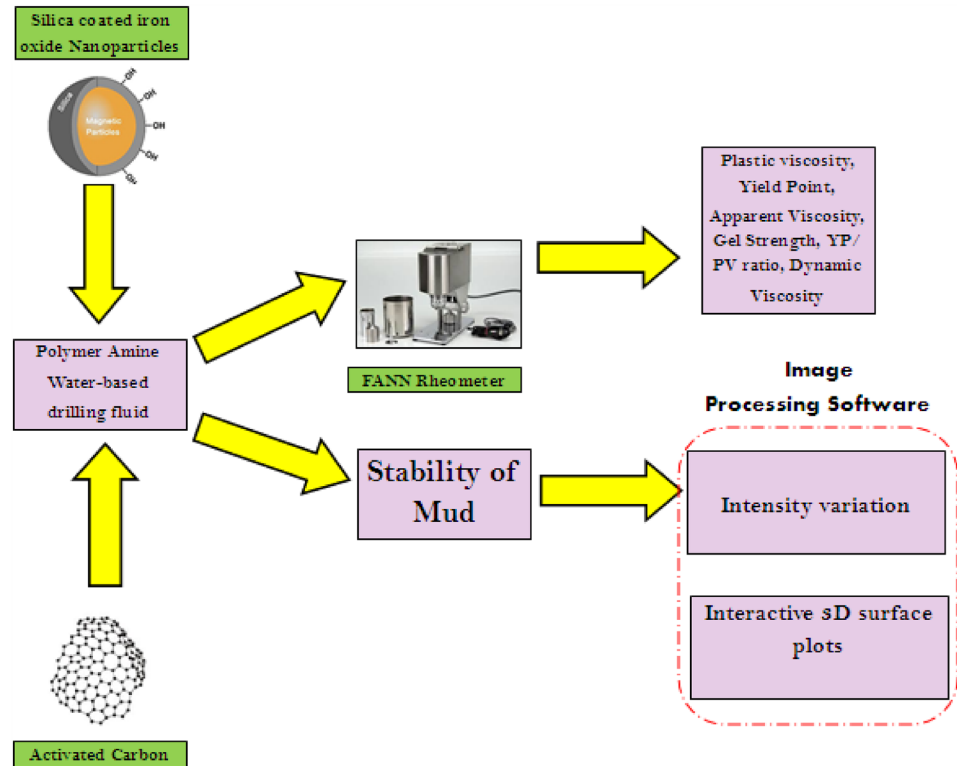
Table 2 Different samples under observation and their weight percentages

Name	Particle	Sample concentration
Sample 1	Activated carbon	0.25 wt. %
Sample 2	Activated carbon	0.50 wt. %
Sample 3	Silica-coated iron oxide nanoparticles	0.25 wt. %
Sample 4	Silica-coated iron oxide nanoparticles	0.50 wt. %

Rheological properties

All the rheological parameters were measured using FANN 286 rheometer manufactured by Fann Instrument Company, Houston, Texas, USA. The rheological analyses are performed at ambient condition of 27 °C. Furthermore, each rheological parameter is recorded thrice using FANN 286 rheometer, and the average measurement is reported in the study. The accuracy of the six-speed rheometer used in this study is ± 0.5 of dial measurement. Eqs. (1, 2 and 3) are used to measure the rheological properties of the drilling fluid in this study (Ali Rafieefar et al. 2021).

$$\text{Plastic viscosity cP } \theta_{600} - \theta_{300} \tag{1}$$

Yield Point lb/100ft^2 $\theta_{300} - PV$ (2)

Apparent Viscosity cP $\dfrac{\theta_{600}}{2}$ (3)

θ_{600} and θ_{300} are the dial measurements obtained from FANN 286 rheometer. The gel strength is recorded at 10 s interval for each fluid system under observation.

Results and discussion

Mud weight

Mud weight (MW) or usually denoted as mud density is a vital feature during any drilling activity. This parameter acts as a primary barrier; hence, the majority of the drilling problems are related to this factor (Fattah and Lashin 2016; Ismail et al. 2020). To effectively determine the effect of activated carbon and nanoparticles on the salt polymer amine water-based drilling mud, mud weight is the first parameter that was investigated. The expected mud weight for this mud system was 8.6 ppg, which was provided by the service operator. It was observed that no substantial changes in mud weights were observed with the addition of particles as shown in Fig. 3. A narrow range of variation was witnessed with the addition of these particles. Sample 1 and Sample 2 that are prepared from the activated carbon demonstrate an increase of 0.2 ppg MW from the operator provided MW. Sample 3 and Sample 4, which are prepared using the nanoparticles, show an increase of 0.1 ppg from the expected MW. These MW are not high enough to induce fractures or damage the formation. Hence, these particles are effective in maintaining the desired mud density.
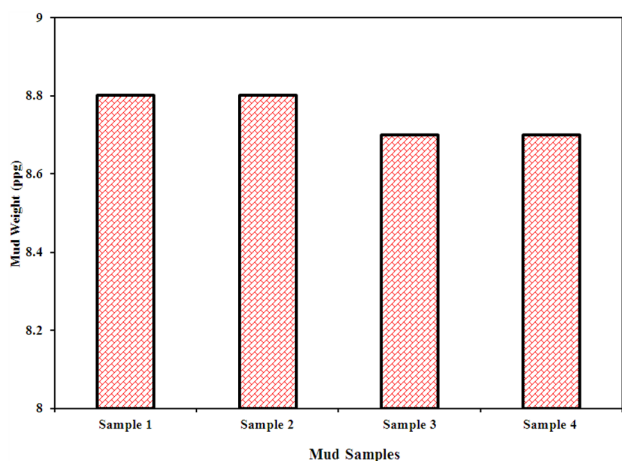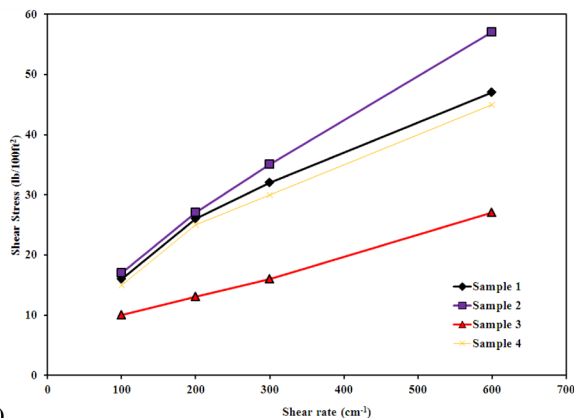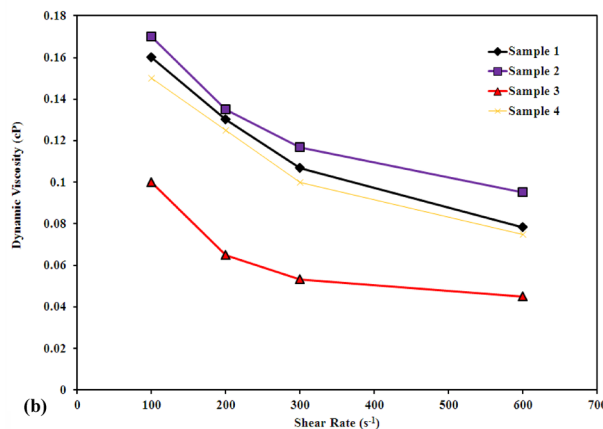
Rheogram of all the samples

Figure 4a shows the rheogram of all the samples in this study. Rheogram describes the flow comportment of any fluid (Jain et al. 2016). This curve consists of a relationship between the shear stress and shear rate, and classifies the fluid either as Newtonian or non-Newtonian in nature (Jain et al. 2016). A linear relationship shows the Newtonian characteristics in the fluid system, whilst a non-linear curve demonstrates non-Newtonian behaviour with either shear thinning or shear thickening properties. All the samples in the study reveal pseudo-plastic or shear thinning behaviour. Moreover, an increase in shear stress was observed with an increase in particle concentration. The maximum shear stress was witnessed in Sample 2. This sample comprises maximum concentration of activated carbon. On the other hand, the minimum shear stress was noted in Sample 3, which consists of the least weight percentage of silica-coated iron oxide nanoparticles.

The rheogram results were also validated with dynamic viscosity results that are represented in Fig. 4b. An increase in shear rate corresponds to the decrease in dynamic

(a)

Fig. 4 **a** Rheogram **b** dynamic viscosity of all the samples in the study

Fig. 3 Mud weight of all the sample in this study

viscosity in all the samples. At low shear rates, the flocculation of the particles and the aggregation of the polymer result in higher shear viscosity. However, as the shear rate increases, the particles and the polymers align in the direction of flow, which eventually reduces the drag force. During pumping and mixing, it is desirable to have fluid that demonstrates low viscosity (Jain et al. 2016). A complete opposite characteristics should be there when the same fluid returns to the surface.

Rheological properties

Figure 5 shows the rheological parameters of all the samples in this article. Figure 5a shows the plastic viscosity (PV) of activated carbon and silica-coated iron oxide nanoparticles. This feature of drilling fluid usually increases with an increase in solid content in the fluid system (Aftab et al. 2016). It is the friction that arises between the different fluid layers or between the solid particle and the fluid layer (Elkatatny 2019). Higher values of PV will develop several problems like high swab and surge pressure, high

equivalent circulation density and high probability of pipe sticking (Aftab et al. 2016). The plastic viscosity of the base mud was 13 cP. After the addition of the particles in the base mud system, an improvement in PV was recorded. The Sample 2 maintained the PV in the desired operating range of (20–29 cP). This sample comprises the highest weight percentage of activated carbon. In the remaining samples, PV was on the lower side. Sample 4, which comprises a higher weight percentage of nanoparticles (NP) shows higher PV value as compared with its lower weight percentage Sample 3. Similar trend was witnessed in Sample 1 and Sample 2. Overall, it was observed that as the concentration of the studied particles increases in the fluid, PV of the system increases. The improvement in PV will eventually assist in cutting transportation mechanisms and will eradicate problems associated with sticking of drill pipe and re-drilling of the formation (Elkatatny 2019).

Figure 5b shows the yield point (YP) of all the samples. YP is denoted as the capability of drilling fluids to carry the drilled cutting up to the surface (Ismail et al. 2020). The presence of electrical charges on the exterior side of
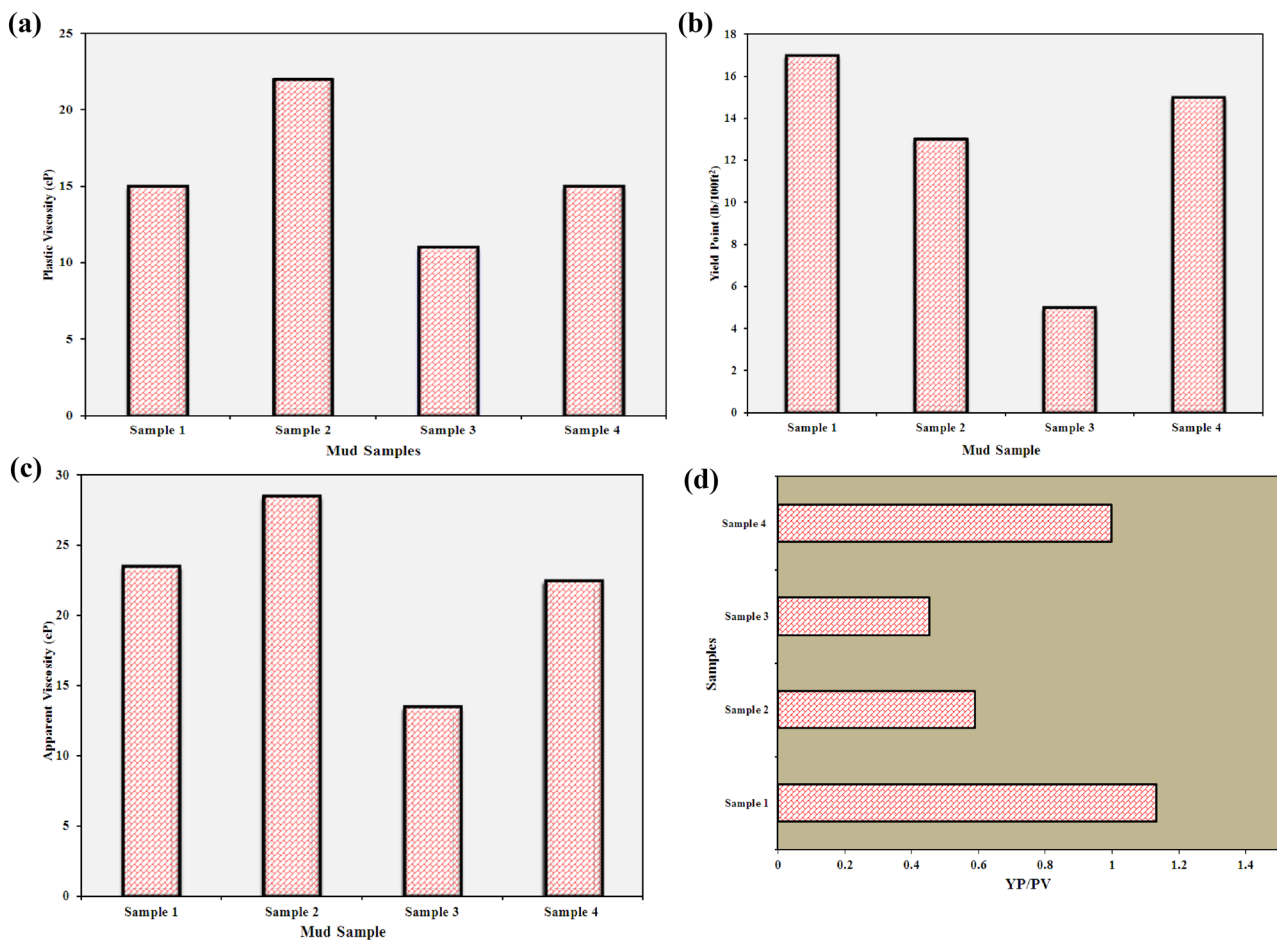

Fig. 5 Rheological properties of all the samples **a** plastic viscosity **b** yield point **c** apparent viscosity **d** ratio of yield point to plastic viscosity

the particle gives rise to electrochemical forces that ultimately give rise to flow resistance in fluids (Ali Esfandyari Bayat et al. 2018). The YP for the base mud system was 10 lb/100ft^2. An improvement in the YP was observed in samples 1, 2 and 4. The maximum YP was observed in sample 1 that consists of activated carbon. Fluids that yield higher YP are more effective in terms of lifting and carrying the drilled cutting up to the surface.

Figure 5c represents the apparent viscosity (AV) of all the samples in the study. The feature of drilling fluid is extremely crucial as it ensures the thixotropic characteristics of drilling muds (Aftab et al. 2016). An increase in AV was observed in Samples 2 and 4 as the concentration of the particles increased. The maximum AV was observed in Sample 2, which consisted of activated carbon. The improvement was because of the hydrophobic nature of activated carbon. Furthermore, as the solid content increased in Samples 2 and 4, the increase in viscosity in these fluid systems was recorded. Figure 5d represents the ratio between the yield point and plastic viscosity (YP/PV) of all the systems in this study. Field experience shows that if the ratio yield point-to-plastic viscosity is equal to $0.75-1 \frac{lb/100ft^2}{cP}$, then that fluid demonstrates efficient cutting carrying capacity and is effective in hole-cleaning process (Zhihua Luo et al. 2017). During this study, fluid samples 1 and 4 were efficient in terms of maintaining this ratio. This clearly indicates that using either activated carbon or silica-coated iron oxide nanoparticles will effectively clean the hole and minimise the possibility of pipe sticking problems. However, concentration of these particles in the drilling fluid is the key parameter in achieving the desired hole-cleaning properties.

Gel strength of the samples

Gel strength (GS) is another important feature of drilling fluid, which represents the capability of the fluid to ensure the suspension of drill cutting under static conditions (Ali Esfandyari Bayat et al. 2018). It is present in the drilling fluid because of the electrochemical attraction within any fluid system (Ali Esfandyari Bayat et al. 2018). Figure 6 shows the 10 s GS for all the samples. The GS that was recorded for the base mud system was 9 lb/100ft^2. It was observed that Samples 1 and 3 that comprise lower concentrations of activated carbon and NPs show similar magnitude and classified as flat rheology. However, when the weight percentage of the particles in the system increased, a corresponding increase in GS was also recorded. The highest GS measured was in Sample 2, which consisted of maximum concentration of activated carbon. An abnormal increase in GS is usually undesirable as it requires higher pumping pressure to break the GS and to initiate the circulation (Elkatatny 2019). In this case, no such irregularity was witnessed in any of the samples.
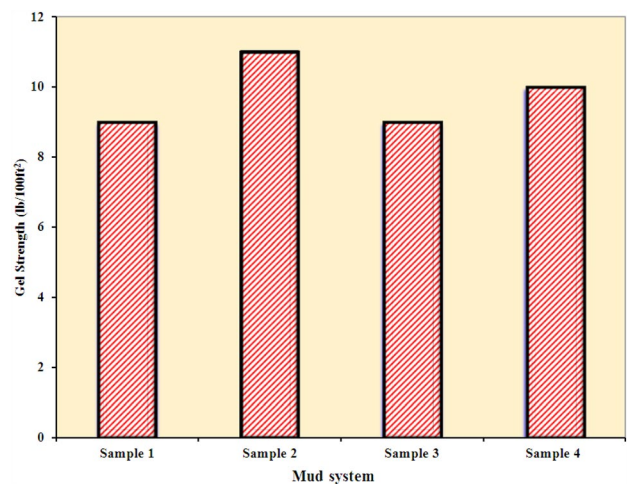

Fig. 6 Effect of activated carbon and silica-coated iron oxide nanoparticles on the gel strength (recorded at ambient condition)

Stability of the mud systems

Figure 7a–d shows the stability of the mud systems observed on two consecutive days. The stability of each mud system was transformed to intensity profile, and the settling of the particles was studied. For the first time, the stabilities of mud systems were observed using these profile plots. Figure 7a shows the intensity profile of Sample 2. This sample comprises 0.5 wt. % of activated carbon in the mud system. According to the Day 1 intensity profile plot, it was observed that settling of solid particles in this system started rapidly. At the top of the test tube, we observed higher intensity regions. This clearly indicates towards the liquid region from which light can easily pass or be transmitted. Towards the lower end of the test tube, and as the distance increased from the top, it was witnessed that intensity decreased, which specified the presence of solid particles. Moreover, an inversely proportional trend between distance and intensity was recorded in this sample. On Day 2 of the observation, it was detected that the area for the high intensity region prolonged further into the test tube and the lower intensity region got smaller in area. This clearly indicates that solid particles move deeper into the test tube.

Figure 7b represents the Sample 1 that comprises lower concentration of activated carbon. The solid additives are distributed equally throughout the test tube. The intensity profile plot clearly demonstrates a horizontal trend in the test tube. There are some regions where light intensity drops significantly. These are the areas that represent the higher concentrations of the solid additives that are either flocculates or are not properly dispersed. Same sample when analysed on Day 2 showed no substantial changes in the intensity of the test tube. There were some regions where intensity dropped rapidly. In these areas, solid particles are

Fig. 7 **a–d** Intensity profiles measuring the stability of mud at day 1 and day 2 **a** sample 2 **b** sample 1 **c** sample 4 **d** sample 3
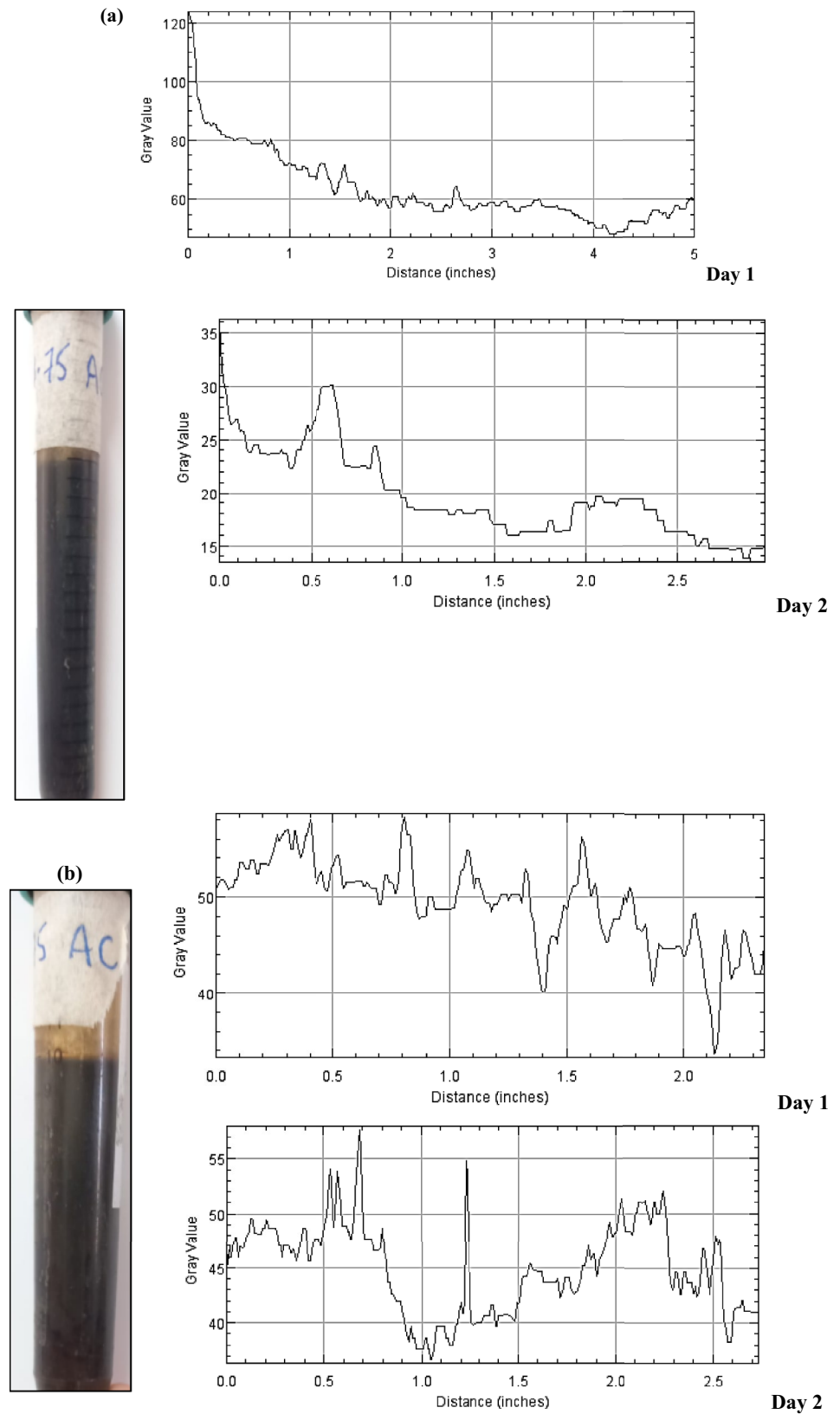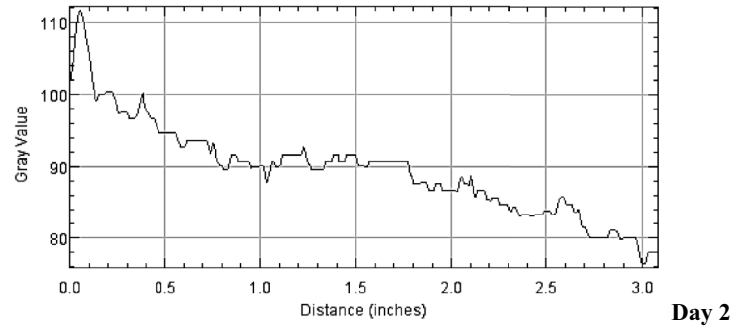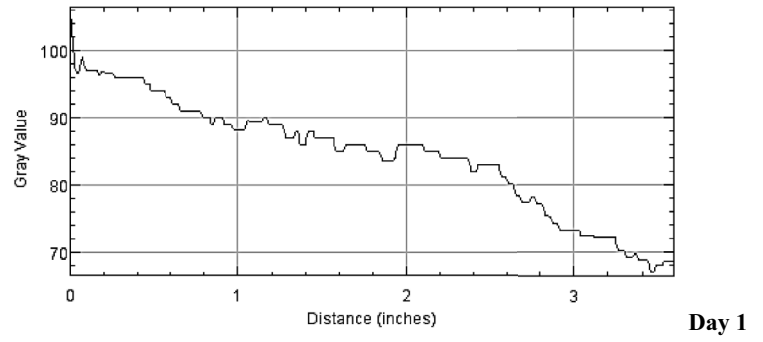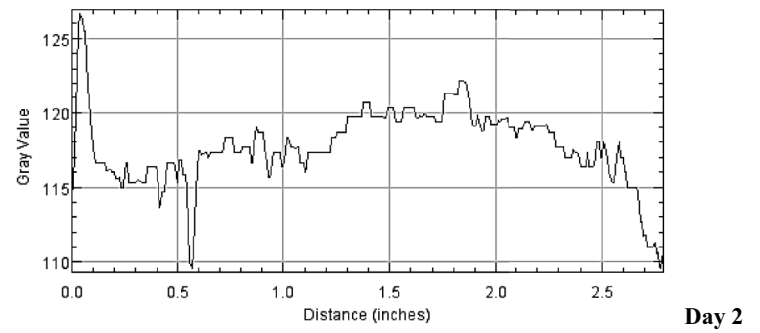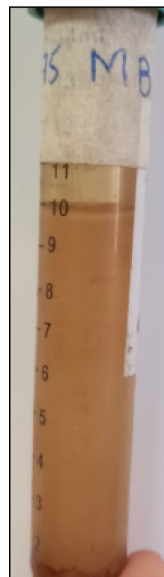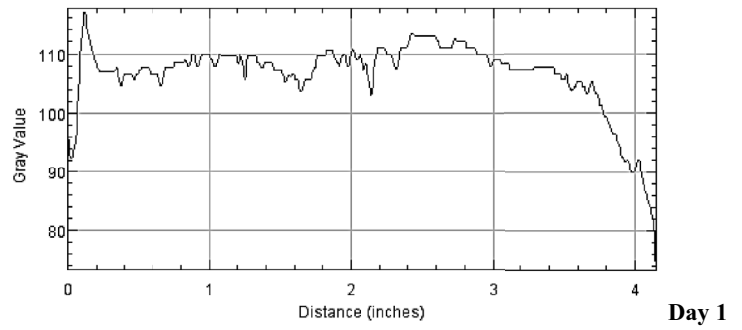
Fig. 7 (continued)

higher in concentration and they will eventually settle down if no movement is provided to the sample.

Figure 7c shows the stability of Sample 4, which consists of 0.5 wt. % of silica-coated iron oxide nanoparticles. The intensity of the test tube throughout its length is on the higher side. This analysis indicates that the particles in this mud system are well dispersed and no coagulation is observed. It starts to get reduced towards the bottom side of the test tube. However, the intensity was still on the higher side. On Day 2 of the observation, a sudden increase in the intensity profile was recorded. This increase was mainly because of the separation of the water phase from the mud system. However, still the overall intensity profile was on the higher side and it started to drop at the bottom side of the test tube. This drop is mainly as a result of solid particles that separate out and are falling under the action of gravity. The nano-sized particles of the additive are not substantial in size to create an impact on the intensity. Hence, it was on the higher side.

Figure 7d shows the intensity profile for Sample 3 that comprises 0.25 weight percentage of nanoparticles. The particles are well dispersed with no signs of coalescences. The intensity peaks throughout the course of the test tube are on the higher side. This clearly demonstrates that the particles are not able to form any flocculation and they are dispersed all the way through the test tube. The negative outer charge of a nanoparticle is forming a shield that prevents the merging of the particles. On Day 2 of the stability test, a strong peak was observed at the distance of 0.1 in. This is mainly due to the separation of water from the mud system. The lower density of water takes it to the top of the test tube where it is able to increase the intensity profile. At a distance of 0.58, the intensity rapidly decreases. This might be due to the accumulation of some particles at this point in the test tube. Nevertheless, apart from that point, the intensity profile was similar in nature throughout the entire length of the test tube. This demonstrates an even distribution of particle with no effect of coagulation.

Stability test on day 5

The intensity profiles for all the mud samples were also recorded on Day 5. Figure 8a–d shows these profiles for each sample. According to Fig. 8a, it was observed that the higher concentration of activated carbon was not feasible in terms of stability. Substantial reduction in intensity peak was recorded, which clearly indicates towards the settling of solid particles. The activated carbon interaction with the mud system was in the opposite manner, and flocculation throughout the test tube was noted through the intensity profile plot. The concentration of activated carbon became half in Sample 1, and it was observed that the intensity profile also changed significantly as shown in Fig. 8b. The

top region profile was on the higher side, which showed the dispersion of the particles. However, towards the later end of the test tube, the profile drops, which corresponds to the settling of the solid particle under the action of gravity. Figure 8c demonstrates the profile for higher concentration of nanoparticles. The liquid phase that was separated out on Day 2 gets higher in volume, which can be observed by an initial larger peak. Moving down the test tube, no substantial changes in peak were recorded, and the behaviour was similar to Day 2. It can be concluded that this sample was quite stable throughout the experimentation. This similar behaviour was also witnessed in a sample that is having lower concentration of silica-coated iron oxide nanoparticles as demonstrated in Fig. 8d.

Interactive 3d surface plot for day 5 sample

Figure 9a–d shows the interactive 3D surface plots for the Day 5 samples in the study. These plots show the intensity within the test tube. Figure 9a represents the interactive 3D plot for Sample 2. This sample consists of a higher weight percentage of activated carbon. On Day 5, it is evident that the intensity decreases towards the bottom of the test tube. The higher intensity region as indicated with blue colour is mainly because of the liquid phase, whilst the greenish colour indicates lower intensity due to the settling of particles at the bottom. Overall, the intensity of the test tube is on the lower side because of the higher concentration of activated carbon. Figure 9b depicts the interactive 3D surface plot for Sample 1 that comprises the least concentration of activated carbon. The overall intensity in the test tube is on the higher side as compared with Sample 2. However, a similar trend as observed in Sample 2 is also detected in this sample. Nevertheless, the intensity at the top of the test tube is higher. This clearly indicates that the separation of water from this sample is higher in volume as compared with Sample 2. Figure 9c represents the Sample 4 3D surface plot. This sample has the higher weight % of silica-coated iron oxide nanoparticles. The overall intensity is on the higher side as compared with Samples 1 and 2. However, some settling of the solid particles is observed with the decrease in intensity profile. On the contrary, when the concentration of the nanoparticles decreases as in the case of Sample 3, the surface plot as indicated in Fig. 9d demonstrates a linear trend with no high fluctuations. This clearly indicates that this sample does not suffer any major stability change after five days. However, some de-phase was witnessed at the top part of the test tube with a higher intensity peak. This shows that the liquid phase from the mud separates out and moves to the top.
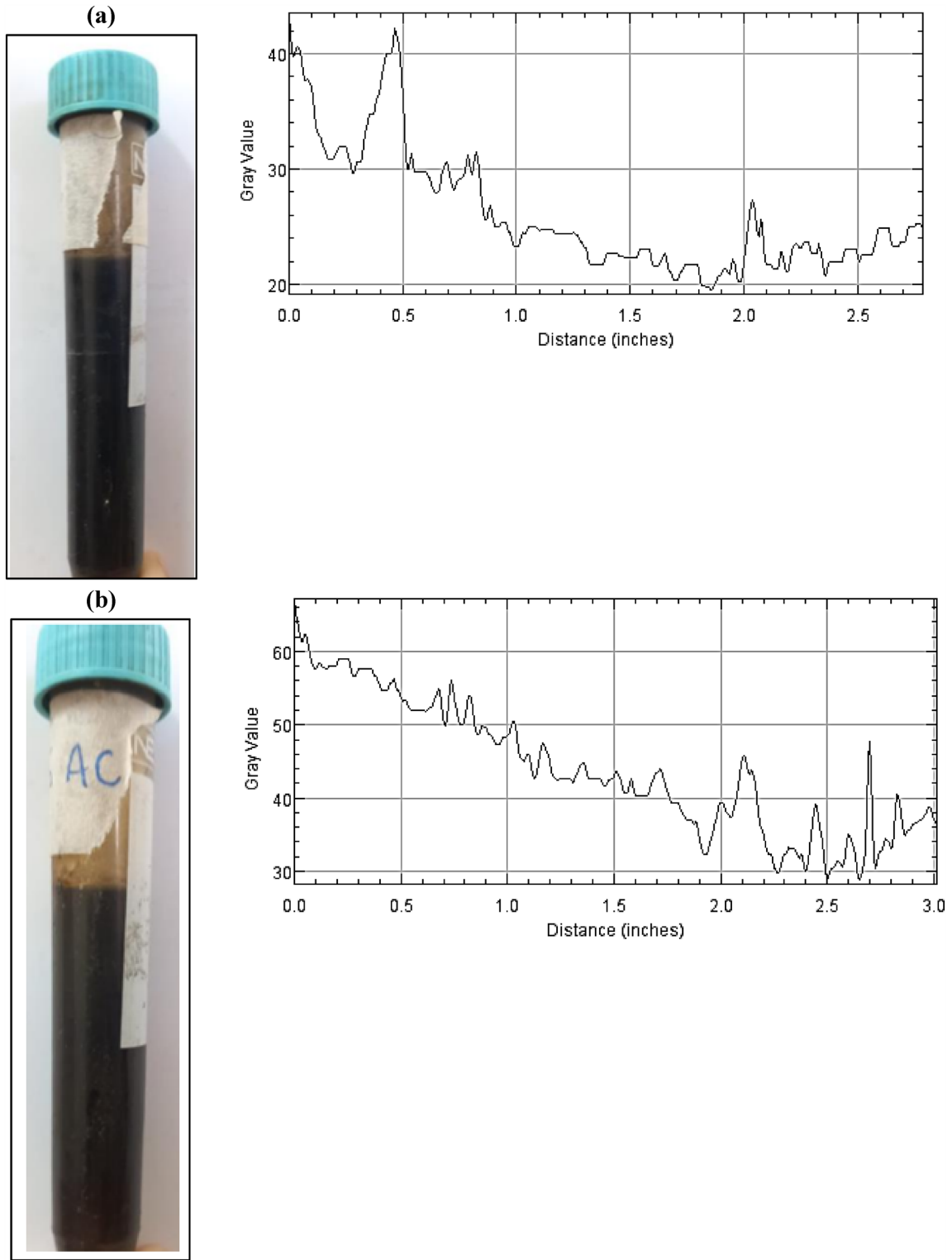
Fig. 8 Intensity profile for the for different mud system obtained at day 5 **a** sample 2 **b** sample 1 **c** sample 4 **d** sample 3
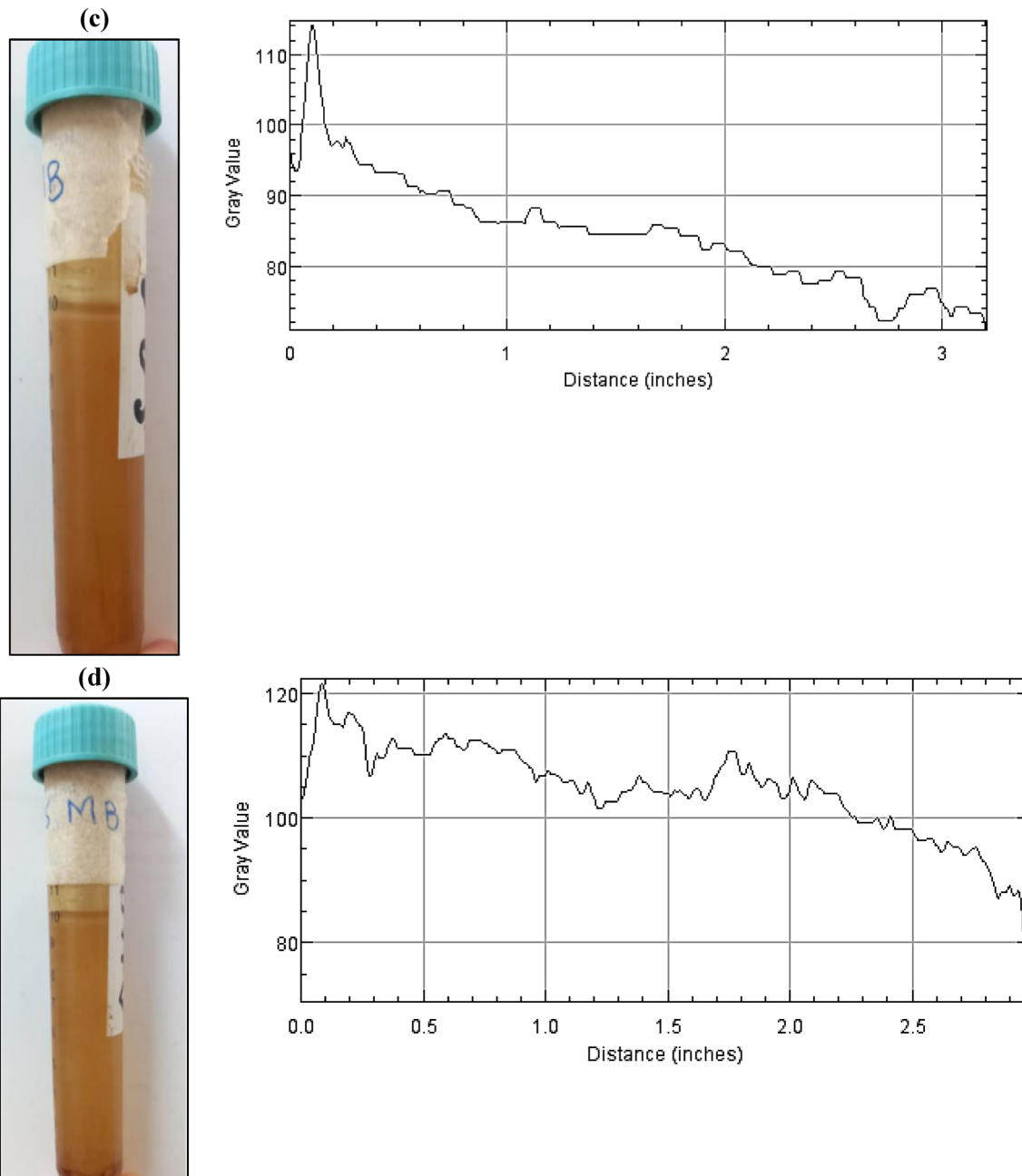
(c)

(d)

Fig. 8 (continued)

Previous studies

The influence of activated carbon on the rheological behaviour of water-based drilling mud was also investigated by (Mahto 2013). Slight improvements in rheological properties were observed with the addition of 3% of this particle in the base mud system. Moreover, when compared to conventional additives like calcium carbonate (CaCO$_3$), it was observed that this improvement was achieved at very less concentration (Mahto 2013). On the other hand, no application of silica-coated iron oxide nanoparticles in drilling mud exists in literature. However, the iron oxide particle as a separate entity is used by researchers in drilling muds (Alvi et al. 2020). The agglomeration of this particle is utterly responsible for increase in gelation and viscosity (Alvi et al. 2020). Moreover, literatures lack the comparison of these particles. Therefore, it was the main core objective of this study.
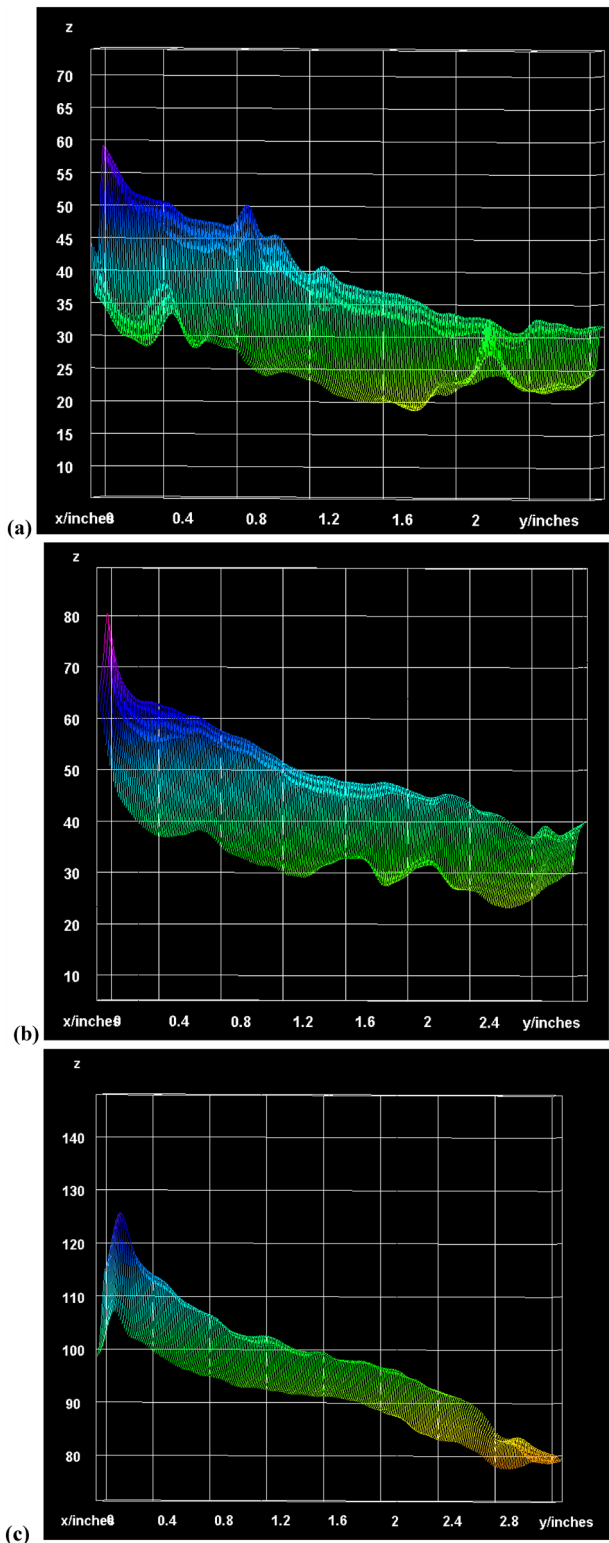
(a)

(b)

(c)

(d)

Fig. 9 (continued)

Fig. 9 **a–d** 3D interaction surface plot **a** sample 2 **b** sample 1 **c** sample 4 **d** sample 3

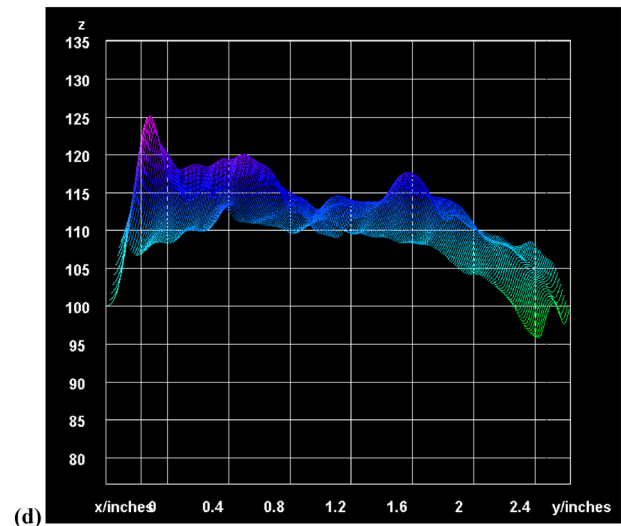## Conclusion

In the current study, for the first time, the rheological comparison is done between silica-coated iron oxide nanoparticles and activated carbon. Additionally, for the first time, stability of the mud system was observed with the help of intensity profile plots. The following results were gathered based on the experimental investigation:

1. No substantial changes in mud weight were recorded after the addition of both particles. The mud weight was close to the base mud weight provided by the operator.
2. All the samples demonstrate shear thinning characteristics, with dynamic viscosity reduces as shear rate increases.
3. Samples that consist of activated carbon exhibit rheological properties in the desired operating range. These samples showed good cutting carrying capacity.
4. No abnormal changes in gel strength were recorded. All samples showed GS closer to base mud system.
5. According to intensity profile plots, the sample with the least concentration of activated carbon was the most stable sample. No substantial change in stability was recorded after two days of experiment.
6. The silica-coated iron oxide nanoparticle starts to dephase on Day 1, and separation was visible on Day 2.
7. On Day 5, each sample experiences either settling of solids or dephasing problems as indicated in surface plots.

Springer

Declarations

References

Abdo J, Haneef MD (2013) Clay nanoparticles modified drilling fluids for drilling of deep hydrocarbon wells. Appl Clay Sci 86:76–82

Adnan Aftab MA, Sahito MF, Mohanty US, Jha NK, Akhondzadeh H, Azhar MR, Ismail AR, Keshavarz A, Iglauer S (2020) Environmental friendliness and high performance of multifunctional tween 80/ZnO-nanoparticles-added water-based drilling fluid: an experimental approach. ACS Sustain Chem Eng 8(30):11224–11243

Aftab AA, Ismail AR, Khokhar S, Ibupoto ZH (2016) Novel zinc oxide nanoparticles deposited acrylamide composite used for enhancing the performance of water-based drilling fluids at elevated temperature conditions. J Petrol Sci Eng 146:1142–1157

Aftab AA, Ismail AR, Ibupoto ZH, Akeiber H, Malghani MG (2017) Nanoparticles based drilling muds a solution to drill elevated temperature wells: a review. Renew Sustain Energy Rev 76:1301–1313

Ahmadi SAR, Kalaee MR, Moradi O et al (2021) Core–shell activated carbon-ZIF-8 nanomaterials for the removal of tetracycline from polluted aqueous solution. Adv Compos Hybrid Mater 4:1384–1397

Al-Ansari A, Parra C, Abahussain A, Abuhamed AM, Pino R, El Bialy M, Mohamed H , and Carlos L. (2017). Reservoir drill-in fluid minimizes fluid invasion and mitigates differential stuck pipe with improved production test results. SPE Middle East Oil & Gas Show and Conference. Manama, Kingdom of Bahrain.

Al-Arfaj MK, Amanullah M, Sultan AS, Hossain E, Abdulraheem A (2014). Chemical and mechanical aspects of wellbore stability in shale formations: a literature review. Abu Dhabi International Petroleum Exhibition and Conference, Abu Dhabi, UAE, SPE.

Al-saba MT, Al Fadhli A, Marafi A, Hussain A, Bander F, Al Dushaishi MF (2018). Application of nanoparticles in improving rheological properties of water based drilling fluids. Paper presented at the SPE Kingdom of Saudi Arabia Annual Technical Symposium and Exhibition. SPE. Dammam, Saudi Arabia.

Ali Rafieefar FS, Hashemi A, Bazargan AM (2021) Rheological behavior and filtration of water-based drilling fluids containing graphene oxide: experimental measurement, mechanistic understanding, and modeling. ACS Omega 6(44):29905–29920

Alvi MA, Belayneh M, Bandyopadhyay S, Minde MW (2020) Effect of iron oxide nanoparticles on the properties of water-based drilling fluids. Energies 13:6718

Asab G, Zereffa EA, Abdo ST (2020) Synthesis of silica-coated fe3o4 nanoparticles by microemulsion method: characterization and evaluation of antimicrobial activity. Int J Biomater 2020:4783612

Azeem Rana TAS (2022) An investigation of polymer-modified activated carbon as a potential shale inhibitor for water-based drilling muds. J Pet Sci Eng 216:110763

Babay S, Mhiri T, Toumi M (2015) Synthesis, structural and spectroscopic characterizations of maghemite γ-Fe2O3 prepared by one-step coprecipitation route. J Mol Struct 1085:286–293

Bayat AE, Moghanloo PJ, Piroozian A, Rafati R (2018) Experimental investigation of rheological and filtration properties of water-based drilling fluids in presence of various nanoparticles. Colloids Surf A 555:256–263

Begum MH, Rahman ASA, Molla MR et al (2023) Preparation and characterization of activated carbon from paper mill sludge by chemical activation: a waste management approach. Int J Environ Sci Technol 20:2757–2770. https://doi.org/10.1007/s13762-022-04169-w

Chen Z, Huang Y (2021) Preparation and performance of fumed silica-stabilized epoxy resin pickering emulsion for basalt fiber–sizing agents. Adv Compos Hybrid Mater 4:1205–1214

Chen H, Yang M, Qiao D, Zhang X, Zhang H (2022) Temperature effects on thermal transport at the graphene-liquid interface. Eng Sci 20:296–305

Cheng K, Zou L, Chang B et al (2022) Mechanically robust and conductive poly(acrylamide) nanocomposite hydrogel by the synergistic effect of vinyl hybrid silica nanoparticle and polypyrrole for human motion sensing. Adv Compos Hybrid Mater 5:2834–2846

Cheraghian G (2021) Nanoparticles in drilling fluid: a review of the state-of-the-art. J Market Res 13:737–753

Choi S, Raja IS, Selvaraj AR et al (2023) Activated carbon nanofiber nanoparticles incorporated electrospun polycaprolactone scaffolds to promote fibroblast behaviors for application to skin tissue engineering. Adv Compos Hybrid Mater. https://doi.org/10.1007/s42114-022-00608-x

Deng Z, Deng Q, Wang L et al (2021a) Modifying coconut shell activated carbon for improved purification of benzene from volatile organic waste gas. Adv Compos Hybrid Mater 4:751–760

Deng Z, Sun S, Li H et al (2021b) Modification of coconut shell-based activated carbon and purification of wastewater. Adv Compos Hybrid Mater 4:65–73

Deng Z, Zhang Q, Deng Q et al (2022) Modification of coconut shell activated carbon and purification of volatile organic waste gas acetone. Adv Compos Hybrid Mater 5:491–503

Duan X, Cheng S, Tao R et al (2022) Synergistically enhanced thermal control ability and mechanical properties of natural rubber for tires through a graphene/silica with a dot-face structure. Adv Compos Hybrid Mater 5:1145–1157

Elkatatny S (2019) Enhancing the Rheological properties of water-based drilling fluid using micronized starch. Arab J Sci Eng 44:5433–5442

Fattah KA, Lashin A (2016) Investigation of mud density and weighting materials efect on drilling fuid flter cake properties and formation damage. J Afr Earth Sci 117:345–357

Fronczak M, Pyrzyńska K, Bhattarai A et al (2019) Improved adsorption performance of activated carbon covalently functionalised with sulphur-containing ligands in the removal of cadmium from aqueous solutions. Int J Environ Sci Technol 16:7921–7932

He Y, Zhou M, Mahmoud MHH et al (2022) Multifunctional wearable strain/pressure sensor based on conductive carbon nanotubes/silk

nonwoven fabric with high durability and low detection limit. Adv Compos Hybrid Mater 5:1939–1950

Heidarinejad Z, Dehghani MH, Heidari M et al (2020) Methods for preparation and activation of activated carbon: a review. Environ Chem Lett 18:393–415

Ibrahim Khan KS, Khan I (2019) Nanoparticles: properties, applications and toxicities. Arab J Chem 12(7):908–931

Ismail AR, Mohd NMNA, Basir NF et al (2020) Improvement of rheological and filtration characteristics of water-based drilling fuids using naturally derived henna leaf and hibiscus leaf extracts. J Petrol Explor Prod Technol 10:3541–3556

Jain R, Mahto TK, Mahto V (2016) Rheological investigations of water based drilling fluid system developed using synthesized nanocomposite. Korea-Aust Rheol J 28:55–65

Jung YB, Lee M, Phuoc J, Tran P, Soong Y, Martello D, Chyu M (2011) Effect of nanoparticle-additives on the rheological properties of clay-based fluids at high temperature and high pressure. Am. Assoc. Drill. Eng. 1–4. AADE-11-NTCE-2

Kamath G, Mishra B, Tiwari S, Bhardwaj A, Marar SS, Soni S, Chauhan R (2022) Experimental and statistical evaluation of drilling induced damages in glass fiber reinforced polymer composites – taguchi integrated supervised machine learning approach. Eng Sci 19:312–318

Kosheleva RI, Mitropoulos AC, Kyzas GZ (2019) Synthesis of activated carbon from food waste. Environ Chem Lett 17:429–438

Kuang T, Zhang M, Chen F et al (2023) Creating poly(lactic acid)/carbon nanotubes/carbon black nanocomposites with high electrical conductivity and good mechanical properties by constructing a segregated double network with a low content of hybrid nanofiller. Adv Compos Hybrid Mater. https://doi.org/10.1007/s42114-022-00622-z

Lalji SM, Ali SI, Awan ZUH et al (2021a) A novel technique for the modeling of shale swelling behavior in water-based drilling fluids. J Petrol Explor Prod Technol 11:3421–3435

Lalji SM, Khan MA, Haneef J et al (2021b) Nano-particles adapted drilling fluids for the swelling inhibition for the Northern region clay formation of Pakistan. Appl Nanosci 13:503

Lalji SM, Ali SI, Ahmed R et al (2022a) Influence of graphene oxide on salt-polymer mud rheology and Pakistan shale swelling inhibition behavior. Arab J Geosci. https://doi.org/10.1007/s12517-022-09800-1

Lalji SM, Ali SI, Sohail H et al (2022b) Combine effect of graphene oxide, pure-bore and sodium alginate on rheological and filtration properties and cutting carrying capacity of water-based drilling fluid. Chem Pap 76:6461–6473

Lu JY, Zhong Y, Yin Hu, Qiu Q (2022) The study on activated carbon, magnetite, polyaniline and polypyrrole development of methane production improvement from wastewater treatment. ES Food Agrofor 10:30–38

Mahto V (2013) Effect of activated charcoal on the rheological and filtration properties of water based drilling fluids. Int J Chem Petrochem Technol (IJCPT) 3(4):27–32

Mohan N, Kalam SA, Mahaveerkannan R, Shah M, Yadav JS, Sharma V, Naik PS, Narasimha DB (2022) Statistical evaluation of machining parameters in drilling of glass laminate aluminum reinforced epoxy composites using machine learning model. Eng Sci. https://doi.org/10.30919/es8e716

Mohideen AAM, Saheed MS, Mohamed NM (2019). Multiwalled carbon nanotubes and graphene oxide as nano-additives in water-based drilling fluid for enhanced fluid-loss-control & gel strength. AIP Conference Proceedings.

Qin L, Jing G, Cui N et al (2023) Resveratrol-silica aerogel nanodrug complex system enhances the treatment of sports osteoarthritis by activating SIRT-1. Adv Compos Hybrid Mater 6:3

Samsuri AW, Sadegh-Zadeh F, Seh-Bardan BJ (2014) Characterizationof biochars produced from oil palm and rice husks and their adsorption capacities for heavy metals. Int J Environ Sci Technol 11:967–976

Shao Y, Bai H, Wang H et al (2022) Magnetically sensitive and high template affinity surface imprinted polymer prepared using porous TiO2-coated magnetite-silica nanoparticles for efficient removal of tetrabromobisphenol A from polluted water. Adv Compos Hybrid Mater 5:130–143

Sharma MM, Zhang R, Chenevert ME, Ji L, Guo Q, Friedheim J (2012). New family of nanoparticle based drilling fluids. SPE Annual Technical Conference and Exhibition. SPE. San Antonio, Texas, USA.

Si Y, Li J, Cui B et al (2022) Janus phenol–formaldehyde resin and periodic mesoporous organic silica nanoadsorbent for the removal of heavy metal ions and organic dyes from polluted water. Adv Compos Hybrid Mater 5:1180–1195

Soares SF, Fateixa S, Trindade T et al (2022) A versatile synthetic route towards gelatin-silica hybrids and magnetic composite colloidal nanoparticles. Adv Compos Hybrid Mater 5:884–898

Sun Z, Qu K, Cheng Y, You Y, Huang Z, Umar A, Ibrahim YS, Algadi H, Castañeda L, Colorado HA, Guo Z (2021) Corncob-derived activated carbon for efficient adsorption dye in sewage. ES Food Agroforest 4:61–74

Tiwari Nidhi KS (2022) Impact of current collector on supercapacitive performance of hydrothermally reduced graphene oxide electrode. ES Energy Environ 15:67–75

Turrina C, Oppelt A, Mitzkus M et al (2022) Silica-coated superparamagnetic iron oxide nanoparticles: new insights into the influence of coating thickness on the particle properties and lasioglossin binding. MRS Commun. 12:632–639

Wang P, Song T, Abo-Dief HM et al (2022a) Effect of carbon nanotubes on the interface evolution and dielectric properties of polylactic acid/ethylene–vinyl acetate copolymer nanocomposites. Adv Compos Hybrid Mater 5:1100–1110

Wang P, Yang L, Ling J et al (2022b) Frontal ring-opening metathesis polymerized polydicyclopentadiene carbon nanotube/graphene aerogel composites with enhanced electromagnetic interference shielding. Adv Compos Hybrid Mater 5:2066–2077

Xie K, Wei S, Alhadhrami A et al (2022a) Synthesis of CsPbBr 3/CsPb2Br5@silica yolk-shell composite microspheres: precisely controllable structure and improved catalytic activity for dye degradation. Adv Compos Hybrid Mater 5:1423–1432

Xie W, Yao F, Gu H et al (2022b) Magnetoresistive and piezoresistive polyaniline nanoarrays in-situ polymerized surrounding magnetic graphene aerogel. Adv Compos Hybrid Mater 5:1003–1016

Yan Z, Wang S, Bi J et al (2022) Strengthening waterborne acrylic resin modified with trimethylolpropane triacrylate and compositing with carbon nanotubes for enhanced anticorrosion. Adv Compos Hybrid Mater 5:2116–2130

Yong-Hui Deng C-W, Jian-Hua Hu, Yang W-L, Shou-Kuan Fu (2005) Investigation of formation of silica-coated magnetite nanoparticles via sol–gel approach. Colloids Surf, A 262(1):87–93

Zhang Z, Liu M, Ibrahim MM et al (2022) Flexible polystyrene/graphene composites with epsilon-near-zero properties. Adv Compos Hybrid Mater 5:1054–1066

Zhihua Luo JP, Wang L, Peizhi Yu, Chen Z (2017) Influence of an ionic liquid on rheological and filtration properties of water-based drilling fluids at high temperatures. Appl Clay Sci 136:96–102

Zhu H, Wang Y, Qu M et al (2022) Electrospun poly(vinyl alcohol)/silica film for radiative cooling. Adv Compos Hybrid Mater 5:1966–1975

مدينة الملك عبدالعزيز
KACST للعلوم والتقنية

Springer

Authors and Affiliations

Shaine Mohammadali Lalji[1] · **Syed Imran Ali[1]** · **Rezwan Ullah[2]** · **Syed Muhammad Ali[3]** · **Yassar Kamal Zia[3]** · **Rizwan Ghauri[4]** · **Abrar Ahmed[5]**

✉ Shaine Mohammadali Lalji
  shaine@neduet.edu.pk

✉ Syed Muhammad Ali
  syed.ali.29@aramco.com

  Syed Imran Ali
  engrimran@neduet.edu.pk

  Rezwan Ullah
  rezwanwazir@gmail.com

  Yassar Kamal Zia
  yassarkamal.zia@aramco.com

  Rizwan Ghauri
  rig00028@students.stir.ac.uk

  Abrar Ahmed
  Abrar.Ahmed@uep.com.pk

[1] Department of Petroleum Engineering, NED University of Engineering & Technology, Karachi, Pakistan

[2] PMAS-AAUR University Institute of Information Technology, Rawalpindi, Pakistan

[3] Exploration & Oil Drilling Engineering Department, Abqaiq, Eastern Province, Kingdom of Saudi Arabia

[4] Department of Computer Science and Management, University of Stirling, Ras Al Khaimah, United Arab Emirates

[5] United Energy Pakistan Limited, Karachi, Pakistan